

PAPER

# $^{51}\text{V}$ -NMR study of charge order induced by cation order in $\delta\text{-Ag}_{2/3}\text{V}_2\text{O}_5$

To cite this article: Y. Kawasaki *et al* 2017 *J. Phys.: Conf. Ser.* **807** 062001

View the [article online](#) for updates and enhancements.

## Related content

- [\$^{51}\text{V}\$ -NMR study of low-temperature phase in  \$\text{Ag}\_{2/3}\text{V}\_2\text{O}\_5\$](#)   
Y Kawasaki, R Morioka, Y Kishimoto *et al.*
- [\$^{51}\text{V}\$ -NMR study of the Kagome staircase compound  \$\text{Co}\_3\text{V}\_2\text{O}\_8\$](#)   
V Ogloblichev, K Kumagai, A Yakubovsky *et al.*
- [\$^{51}\text{V}\$ -NMR Study of Honeycomb Lattice Antiferromagnet  \$\text{InCu}\_{2/3}\text{V}\_{1/3}\text{O}\_3\$](#)   
Y Fujii, D Takahashi, Y Kubo *et al.*



**IOP | ebooks™**

Bringing you innovative digital publishing with leading voices to create your essential collection of books in STEM research.

Start exploring the collection - download the first chapter of every title for free.

# $^{51}\text{V}$ -NMR study of charge order induced by cation order in $\delta\text{-Ag}_{2/3}\text{V}_2\text{O}_5$

Y. Kawasaki<sup>1</sup>, R. Morioka<sup>1</sup>, Y. Kishimoto<sup>1</sup>, K. Nakamura<sup>1</sup>,  
K. Nishiyama<sup>2</sup>, T. Koyama<sup>2</sup>, T. Mito<sup>2</sup>, T. Baba<sup>3</sup>, T. Yamauchi<sup>3</sup>,  
M. Isobe<sup>4</sup> and Y. Ueda<sup>5</sup>

<sup>1</sup> Graduate School of Science and Technology, Tokushima University, Tokushima 770-8506, Japan

<sup>2</sup> Graduate School of Material Science, University of Hyogo, Hyogo 678-1297, Japan

<sup>3</sup> Institute for Solid State Physics, University of Tokyo, Kashiwa 277-8581, Japan

<sup>4</sup> Max Planck Institute for Solid State Research, D-70569 Stuttgart, Germany

<sup>5</sup> Toyota Physical and Chemical Research Institute, Nagakute, Aichi 480-1192, Japan

E-mail: [kawasaki.yu@tokushima-u.ac.jp](mailto:kawasaki.yu@tokushima-u.ac.jp)

**Abstract.**  $^{51}\text{V}$ -NMR experiments have been performed to investigate the local magnetic and electronic properties of the mixed-valence oxide  $\delta\text{-Ag}_{2/3}\text{V}_2\text{O}_5$ , which shows the novel  $\text{V}^{4+}/\text{V}^{5+}$  charge ordering triggered by Ag ion ordering. We have observed the abrupt loss of  $^{51}\text{V}$ -NMR signal coming from the non-magnetic  $\text{V}^{5+}$ -like ions above  $T_c = 225$  K. It indicates that the majority of V ions are magnetic above  $T_c$  and that the phase transition is accompanied by the charge separation and the charge ordering of  $3d$  electrons on V sites. In the low-temperature phase below  $T_c$ , the nuclear spin-lattice relaxation rate  $1/T_1$  shows the thermal activation-type temperature dependence with the activation energy of about 130 K. It has been clarified that the ground state of this material is the charge ordered one with the spin singlet of  $3d$  electrons on  $\text{V}^{4+}\text{-V}^{4+}$  pair from a microscopic point of view.

## 1. Introduction

Various exotic phenomena due to spin, charge, lattice and orbital degrees of freedom have attracted much attention in strongly correlated electron systems [1]. Among them, the charge ordering is one of the most intriguing and extensively studied phenomena related to the charge degrees of freedom. In the vanadium bronzes  $A_x\text{V}_2\text{O}_5$  ( $A$ : alkali, alkaline-earth or other metals), mixed-valence oxides of  $\text{V}^{4+}$  ( $3d^1$ ) and  $\text{V}^{5+}$  ( $3d^0$ ), the charge ordering may appear in its stoichiometric composition, where the number of  $3d$  electrons could be controlled as a function of  $x$ . The first discovery of the charge ordering in this system has been made on  $\alpha'$ - $\text{NaV}_2\text{O}_5$  [2, 3]. For the last decade, the charge ordering in  $\beta\text{-}A_{1/3}\text{V}_2\text{O}_5$  has been intensively investigated in connection with the superconductivity that appears when the charge ordering is suppressed by applying pressure for  $A = \text{Li}, \text{Na}$  and  $\text{Ag}$  [4, 5]. For example,  $\beta\text{-Na}_{1/3}\text{V}_2\text{O}_5$  shows the successive phase transitions at ambient pressure; the ordering of Na atoms at 242 K, the metal-insulator transition at 135 K and the antiferromagnetic one at 24 K. Various experiments have clarified that the metal-insulator transition is accompanied by the charge ordering or the charge disproportionation [6, 7, 8, 9].



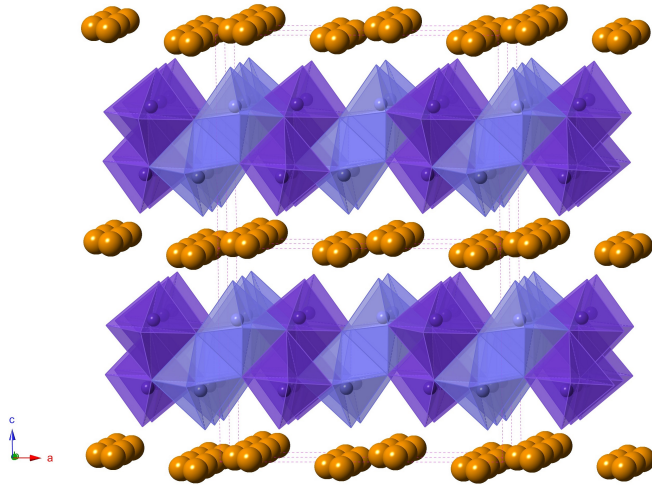


**Figure 1.** Crystal structure of  $\delta\text{-Ag}_{2/3}\text{V}_2\text{O}_5$ , where mauve octahedra, blue octahedra and orange balls represent  $\text{V1O}_6$ ,  $\text{V2O}_6$  and Ag, respectively. (from Ref.[10])

Now, we focus on  $\delta\text{-Ag}_{2/3}\text{V}_2\text{O}_5$ , which shows the novel charge ordering induced by cation ordering [11]. The crystal structure consists of  $\text{V}_2\text{O}_5$  double-trellis layers and Ag ions located between the double-trellis layers (Fig. 1) [11, 12, 13]. There are two V sites denoted as V1 and V2, and each V forms a distorted octahedron at room temperature,  $\text{V1O}_6$  (mauve octahedra in the figure) and  $\text{V2O}_6$  (blue ones). The  $\text{V}_2\text{O}_5$  double-trellis layers are formed by edge/corner-shared  $\text{V1O}_6$  and  $\text{V2O}_6$  octahedra. Ag ions (orange balls) partly occupy one of two nearest-neighboring sites between the double-trellis layers.

Regarding its electromagnetic properties, this oxide shows the first-order transition at around 220 K, accompanied by the jumps in electric resistivity and magnetic susceptibility [11, 13]. The transport properties become more insulating below  $T_c$ , which may be associated with the  $\text{V}^{4+}/\text{V}^{5+}$  charge ordering in the formal valence of  $\text{V}^{4+}/\text{V}^{5+} = 1/2$ . Recently, Baba et al. have revealed that the phase transition is caused by the Ag ion ordering, which triggers the charge ordering [11], where this phenomenon seems to be closely related to the fact that the ratio of  $\text{V}^{4+}/\text{V}^{5+} = 1/2$  is identical to the ratio of Ag vacancies/Ag = 1/2. Interestingly, the phase transition can be supercooled to the lowest temperature by rapid cooling, which may prevent the Ag ion ordering. Below the transition temperature, the magnetic susceptibility shows a broad maximum at around 110 K followed by spin-gapped behavior, in contrast to Curie-Weiss behavior above the transition temperature. These results indicate that the magnetic  $\text{V}^{4+}$  ions have a specific geometrical arrangement required for the spin-gap state and that the geometrical arrangement is closely related to the Ag ion ordering. In this study, we have performed  $^{51}\text{V}$ -NMR measurements to investigate the electromagnetic properties of  $\delta\text{-Ag}_{2/3}\text{V}_2\text{O}_5$ , focusing on the spin-gap behavior in the low-temperature phase below  $T_c$ .

## 2. Experimental

A powder sample of  $\delta\text{-Ag}_{2/3}\text{V}_2\text{O}_5$  was prepared by a solid state reaction method. The detailed preparation method has been reported elsewhere [11]. X-ray diffraction and magnetic susceptibility confirm that the structural and magnetic properties are consistent with the published data [11, 13]. The transition temperature  $T_c$  on warming process for our sample was determined to be 225 K from the inflection point on the  $^{51}\text{V}$ -NMR signal intensity vs. temperature curve, where the signal intensity abruptly decreases as mentioned later.

For NMR, we cooled the sample down to 5.0 K with sufficiently slow rate of 2 K/min and subsequently performed measurements at elevated temperature. The spin-echo signal of  $^{51}\text{V}$  nuclei (the nuclear spin of  $I = 7/2$ ) was observed by the spin-echo method, using a phase-coherent pulsed NMR spectrometer. The  $^{51}\text{V}$ -NMR spectrum was obtained by tracing the

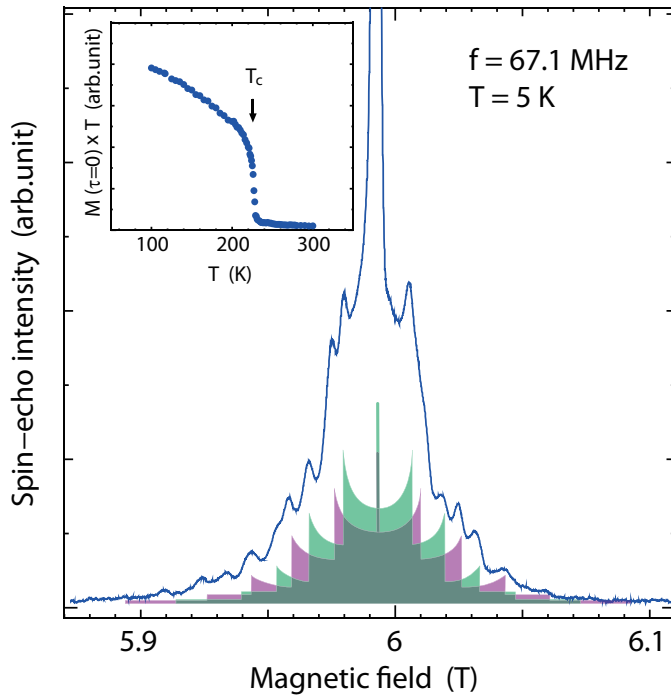


**Figure 2.** Field-swept  $^{51}\text{V}$ -NMR spectrum of  $\delta\text{-Ag}_{2/3}\text{V}_2\text{O}_5$  at 5.0 K. Inset: Temperature dependence of spin-echo intensity multiplied by temperature,  $M(\tau = 0) \times T$ .

spin-echo intensity as a function of external field at the fixed frequency of 67.1 MHz. For the measurements of the nuclear spin-lattice relaxation rate  $1/T_1$ , we used the saturation recovery method. The spin-spin relaxation rate  $1/T_2$  was obtained from the decaying rate of the spin-echo intensity  $M(\tau)$  against the pulse separation  $\tau$  in the spin-echo method. Here, the spin-echo intensity  $M(\tau)$  is expressed by the equation,  $M(\tau) = M(\tau = 0) \exp(-2\tau/T_2)$ .

### 3. Results and discussion

In Fig.2, we show the field-swept  $^{51}\text{V}$ -NMR spectrum measured at the fixed frequency of 67.1 MHz at 5.0 K in the low-temperature phase. The spectrum consists of two typical powder patterns (S1 and S2) for  $^{51}\text{V}$  nuclei with different NQR frequencies, which are indicated by the green and the purple areas, respectively, in the figure. The NQR frequencies for S1 and S2 are estimated to be  $\nu_{Q1} = 0.29$  MHz and  $\nu_{Q2} = 0.43$  MHz, respectively, from the 1st satellite peak positions, where the respective asymmetric parameter is nearly zero for both.

One may consider that S1 and S2 are associated with non-magnetic  $\text{V}^{5+}$ -like ions located at the V1 and V2 sites ( $\text{V1}^{5+}$  and  $\text{V2}^{5+}$ ), although it is unclear whether S1 (S2) comes from  $\text{V1}^{5+}$  or  $\text{V2}^{5+}$  at present. The non-magnetic nature of V ions associated with S1 and S2 is indicated by the facts: (i) the positions of central peak for S1 and S2 are almost same and the corresponding Knight shifts are nearly zero, (ii)  $T_2$ 's for S1 and S2 are comparable, as described in the next paragraph, which indicates that the V ions associated with S1 and S2 are magnetically similar, (iii)  $T_2$ 's for S1 and S2 are long and these values are about a few hundred microseconds, which are comparable to the value of  $T_2 \sim 100 \mu\text{s}$  for the  $\text{V}^{5+}$ -like site in the charge ordered phase of  $\beta\text{-Ag}_{1/3}\text{V}_2\text{O}_5$  [14] and (iv) for both S1 and S2, the signal intensity abruptly decreases at  $T_c = 225$  K (see the inset of Fig. 2, showing the temperature dependence of the spin-echo intensity multiplied by temperature,  $M(\tau = 0) \times T$ ), above which the  $\text{V}^{5+}$ -like ions are expected to be almost absent due to the collapse of the charge separation and charge order. A short nuclear spin-spin relaxation time  $T_2$  may prevent us from clearly observing the  $^{51}\text{V}$ -NMR signal of magnetic  $\text{V}^{4+}$ -like ions.

To examine  $T_2$ 's for S1 and S2, we show the  $^{51}\text{V}$ -NMR spectrum with typical values of  $\tau$  in

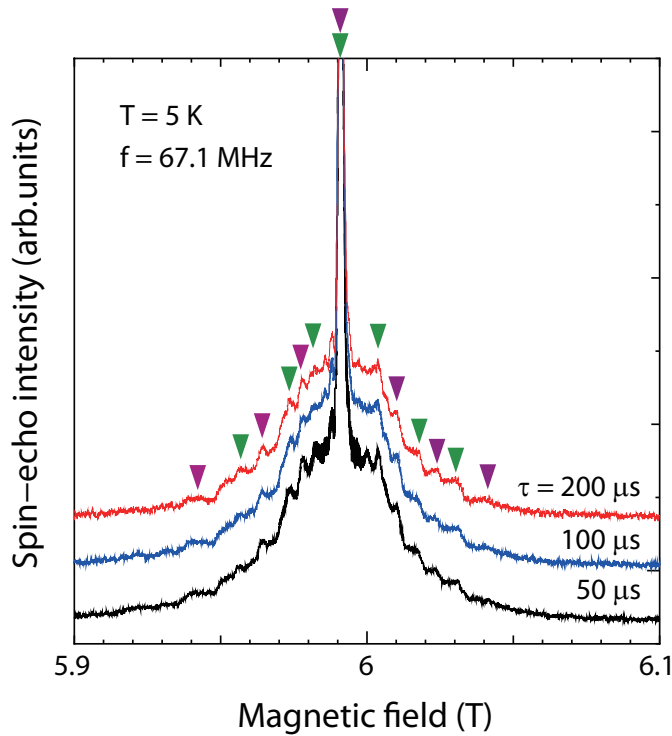


**Figure 3.** Field-swept  $^{51}\text{V}$ -NMR spectra of  $\delta\text{-Ag}_{2/3}\text{V}_2\text{O}_5$  with pulse separation of  $\tau = 50\mu\text{s}$  (black),  $100\mu\text{s}$  (blue) and  $200\mu\text{s}$  (red) at 5 K.

Fig. 3, where the black, blue and red lines represent the data with  $\tau = 50\mu\text{s}$ ,  $100\mu\text{s}$ , and  $200\mu\text{s}$ , respectively. The green and purple down triangles indicate the peak positions in powder pattern for S1 and S2, respectively, in the figure. The relative peak intensity for S1 and S2 is independent of  $\tau$ , which indicates that  $T_2$ 's for S1 and S2 are comparable. The comparable values of  $T_2$ 's for S1 and S2 are also confirmed by the fact that the decay of the spin-echo intensity  $M(\tau)$  against  $\tau$ , measured at the center peak in the spectrum, has a single exponential form.

Next, we go on to the experimental results on the nuclear spin-lattice relaxation rate  $1/T_1$  in  $\delta\text{-Ag}_{2/3}\text{V}_2\text{O}_5$ . In Fig. 4, we show  $(M_0 - M(t))/M_0$  against  $t$  at 105 K as a typical example. Here,  $M(t)$  is the spin-echo intensity, which is proportional to nuclear magnetization  $t$  seconds after the saturation pulse.  $M_0$  is  $M(t)$  in the thermal equilibrium state ( $t \rightarrow \infty$ ). The recovery of  $M(t)$  to the thermal equilibrium state is expressed by

$$\frac{M_0 - M(t)}{M_0} = C_1 \exp\left(-\frac{t}{T_1}\right) + C_2 \exp\left(-\frac{6t}{T_1}\right) + C_3 \exp\left(-\frac{15t}{T_1}\right) + C_4 \exp\left(-\frac{28t}{T_1}\right) \quad (1)$$

for the transition between  $I_z = -1/2$  and  $1/2$  of the nuclear spin  $I = 7/2$ . Here,  $C_1 = 0.019$ ,  $C_2 = 0.0682$ ,  $C_3 = 0.206$ , and  $C_4 = 0.714$  [15]. The solid line in Fig. 4 represents the best fit by Eq.(1) to the data. We note that Eq.(1) reproduces the data for all the measured temperature. It indicates that the observed nuclear spin relaxation is expressed by a single component of  $1/T_1$ , that is to say, the local environments of V1 and V2 sites are magnetically similar, which is consistent with comparable  $T_2$ 's for S1 and S2. The fit enables us to estimate the nuclear spin-lattice relaxation rate  $1/T_1$  at each temperature.

Fig. 5 shows the temperature dependence of the nuclear spin-lattice relaxation rate  $1/T_1$ . The value of  $1/T_1$  decreases exponentially with decreasing temperature below  $T_c$ , followed by the temperature independent behavior below 20 K. The exponential temperature dependence of  $1/T_1$  is confirmed by the Arrhenius plot of the data (inset of Fig. 5). This result indicates the existence of energy gap in magnetic excitation, which is consistent with the spin-singlet state of  $3d$  electrons on  $\text{V}^{4+}\text{-V}^{4+}$  pairs. One may fit the data by the thermal activation-type relation in

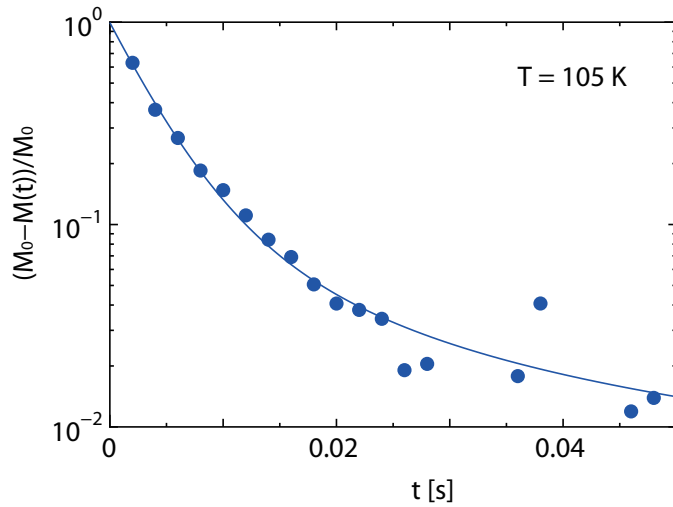


**Figure 4.**  $(M_0 - M(t))/M_0$  vs.  $t$  at 105 K. The solid line indicates the best fit to the data by Eq.(1) (see text).

the temperature range between  $T_c = 225$  K and 30 K, represented by solid lines in Fig. 5 and its inset. This relation is given by

$$\frac{1}{T_1} \propto \exp\left(-\frac{\Delta}{k_B T}\right), \quad (2)$$

where  $\Delta$  is the size of the energy gap and  $k_B$  is the Boltzmann's constant. The size of the energy gap  $\Delta/k_B$  is estimated to be 130 K from the present data, which is comparable to 150 K obtained from the magnetic susceptibility [11]. The deviation from the exponential temperature dependence below 20 K may be due to local fluctuation of  $V^{4+}$  magnetic moments without forming spin singlet. Above  $T_c$ , the value of  $1/T_1$  is slightly smaller than that just below  $T_c$ , which may be related to the small jump in the magnetic susceptibility at  $T_c$ .

#### 4. Conclusion

We have investigated the mixed-valence vanadate  $\delta$ - $\text{Ag}_{2/3}\text{V}_2\text{O}_5$ , which shows the novel  $V^{4+}/V^{5+}$  charge ordering triggered by the Ag ion ordering, from  $^{51}\text{V}$ -NMR measurements. It has been microscopically confirmed that the phase transition is accompanied by the charge separation on V sites at  $T_c$ , above which the  $^{51}\text{V}$ -NMR signal coming from the non-magnetic  $V^{5+}$ -like ions is significantly reduced. In the low-temperature phase below  $T_c$ , the nuclear spin-lattice relaxation rate  $1/T_1$  indicates the existence of energy gap in magnetic excitation, which is consistent with the formation of spin singlet on  $V^{4+}$ - $V^{4+}$  pair. The size of the energy gap is estimated to be about 130 K.

#### References

- [1] Imada M, Fujimori A and Tokura Y 1998 *Rev. Mod. Phys.* **70** 1039
- [2] Isobe M and Ueda Y 1996 *J. Phys. Soc. Jpn.* **65** 1178
- [3] Seo H and Fukuyama H 1998 *J. Phys. Soc. Jpn.* **67** 2602
- [4] Yamauchi T, Ueda Y and Mōri N 2002 *Phys. Rev. Lett.* **89** 057002
- [5] Yamauchi T and Ueda Y 2008 *Phys. Rev. B* **77** 104529
- [6] Yamaura J, Isobe M, Yamada H, Yamauchi T and Ueda Y 2002 *J. Phys. Chem. Solids* **63** 957
- [7] Heinrich M, Krug von Nidda H A, Eremina R M, Loidl A, Helbig Ch, Obermeier G and Horn S 2004 *Phys. Rev. Lett.* **93** 116402
- [8] Nagai S, Hishi M, Kakurai K, Oohara Y, Yoshizawa H, Kimura H, Noda Y, Grenier B, Yamauchi T, Yamaura J, Isobe M, Ueda Y and Hirota K 2005 *J. Phys. Soc. Jpn.* **74** 1297
- [9] Itoh M, Yamauchi I, Kozuka T, Suzuki T, Yamauchi T, Yamaura J and Ueda Y 2006 *Phys. Rev. B* **74** 054434

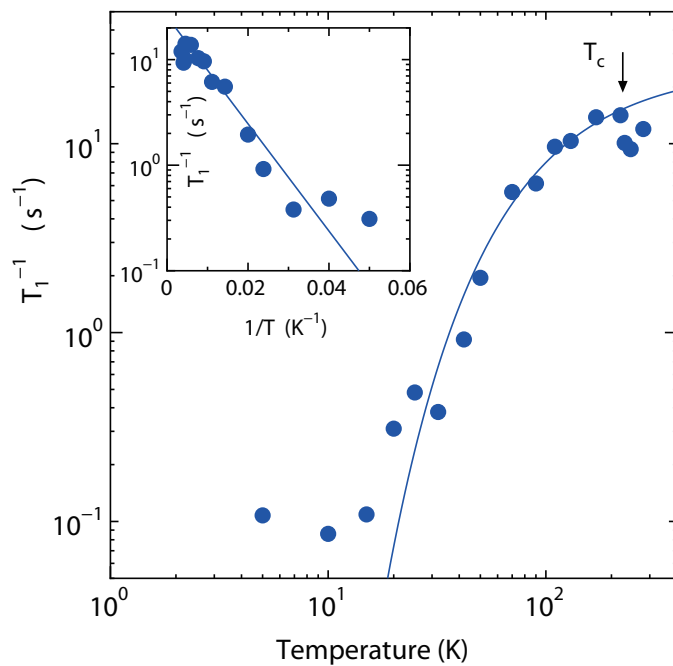


**Figure 5.** The temperature dependence of  $1/T_1$ . Inset: Arrhenius plot of the data shown in the main panel. The solid lines indicate the best fit to the data by the thermal activation-type relation between 20 K and  $T_c$ .

- [10] Kawasaki Y, Morioka R, Nakamura K, Nishiyama K, Koyama T, Mito T, Baba T, Yamauchi T, Isobe M and Ueda Y 2015 *J. Phys.: Conf. Ser.* **592** 012042
- [11] Baba T, Yamauchi T, Yamazaki S, Ueda H, Isobe M, Matsushita Y and Ueda Y 2015 *J. Phys. Soc. Jpn.* **84** 024718
- [12] Andersson S 1965 *Acta Chem. Scand.* **19** 1371
- [13] Onoda M and Arai R 2001 *J. Phys.: Condens. Matter* **13** 10399
- [14] Hisada A, Fujiwara N, Yamauchi T and Ueda Y 2009 *J. Phys. Soc. Jpn.* **78** 094705
- [15] Narath A 1967 *Phys. Rev.* **162** 320